

## **Chapter 2.**

# **Programmable Ligand Controlled Riboregulators of Eukaryotic Gene Expression**

Parts reproduced from: Bayer TS and Smolke CD, **Programmable ligand-controlled riboregulators of eukaryotic gene expression.** *Nature Biotechnology.* 23(3):337-43. (2005).

Recent studies have demonstrated the importance of non-coding RNA elements in regulating gene expression networks.<sup>1,2</sup> We describe the design of a novel class of small trans-acting RNAs that directly regulate gene expression in a ligand-dependent manner. These allosteric riboregulators, which we call antiswitches, are fully tunable and modular by rational design and offer uniquely flexible control strategies by self-regulating to active or inactive forms in response to ligand binding, depending on the platform design. Antiswitches offer “programmable” genetic control and can be tailor-made to control the expression of target transcripts in response to different cellular effectors. Coupled with *in vitro* selection technologies for generating nucleic acid ligand binding species,<sup>3, 4</sup> antiswitches present a powerful platform for designing targeted regulators to program cellular behavior and genetic networks with respect to cellular state and environmental stimuli.

In recent years, *cis* and *trans* RNA elements have become well recognized as important regulators of gene expression. Cells use diverse non-coding RNA-based elements to regulate complex genetic networks such as those involved in developmental timing and circadian clocks.<sup>1, 2</sup> Antisense RNAs are small trans-acting RNAs (taRNAs) that bind to complementary segments of a target messenger RNA (mRNA) and regulate gene expression through mechanisms such as targeting decay, blocking translation, and altering splicing patterns.<sup>5-7</sup> MicroRNAs (miRNAs), small taRNAs that affect either translation or RNA decay by interacting with complementary sequences in mRNA and the genome, are likely widespread in metazoan gene regulation.<sup>8</sup> Small interfering RNAs (siRNAs) and double-stranded RNAs (dsRNAs) are able to precisely target mRNAs and inhibit their expression through the RNA interference (RNAi) pathway in metazoans, and are thought to be part of the cell's host defense system.<sup>9</sup> Ribozymes are RNA molecules exhibiting catalytic function and have been shown to be used by viruses to regulate gene expression.<sup>10</sup> Riboswitches, *cis*-acting metabolite binding structures in mRNAs, control gene expression by modulating translation initiation, disruption of transcriptional termination, or cleavage of mRNA by ribozyme mechanisms.<sup>11-13</sup> Recent studies have demonstrated the prevalence of these RNA-based regulators across diverse groups of organisms from prokaryotes to humans.<sup>14-16</sup>

Researchers have taken advantage of the relative ease with which RNA libraries can be generated and searched to create synthetic RNA-based molecules with novel functional properties. Aptamers are nucleic acid binding species that interact with high

affinity and specificity to selected ligands. These molecules are generated through iterative cycles of selection and amplification known as *in vitro* selection or systematic evolution of ligands by exponential enrichment (SELEX).<sup>3, 4</sup> Aptamers have been selected to bind diverse targets such as dyes, proteins, peptides, aromatic small molecules, antibiotics, and other biomolecules.<sup>17</sup> High-throughput methods and laboratory automation have been developed to generate aptamers in a rapid and parallel manner<sup>18</sup>. Researchers have demonstrated that aptamers can impart allosteric control properties onto other functional RNA molecules. Such allosteric control strategies have been employed to construct and select *in vitro* signaling aptamers, *in vitro* sensors, and *in vitro* allosterically controlled ribozymes.<sup>19-21</sup>

In addition to the widespread occurrence of RNA-based regulator elements in natural systems, researchers have recently described engineered riboregulator systems. Cis-acting RNA elements were described that regulate relative expression levels in *Escherichia coli* from a two gene transcript by controlling RNA processing and decay.<sup>22</sup> In another example, a combined cis/trans riboregulator system was described in *E. coli* in which cis-acting RNA elements mask the ribosome binding site of a transcript, thereby inhibiting translation, and trans-activating RNAs bind to the cis-acting elements to allow translation.<sup>23</sup> Cis-acting elements were recently described that control gene expression in mammalian cells and mice by acting through RNA cleavage and whose activity can be regulated by a small molecule drug and antisense oligonucleotides.<sup>24</sup> Finally, an allosteric aptamer construct was recently described that upon binding the dye tetramethylrosamine, interacts with protein-based transcriptional activators to induce transcription.<sup>25</sup>

Riboregulators present powerful tools for flexible genetic regulation. However, there is a need to couple the ability of RNA-based regulators that can directly target transcripts with allosteric control typically associated with protein-based regulators. We have engineered ligand responsive riboregulators in *Saccharomyces cerevisiae*. These riboregulators, which we call antiswitches, utilize an antisense domain to control gene expression<sup>6</sup> and an aptamer domain to recognize specific effector ligands. Ligand binding at the aptamer domain mediates a change in the conformational dynamics of these molecules that allows the antisense domain to interact with a target mRNA to affect translation. Antiswitches act as programmable genetic switches, affecting target transcripts only in the presence of a specific ligand. We have developed a modular, tunable class of small RNAs that can be used to achieve sensor-based gene expression control. Because antiswitches are designed on a modular platform, in principle these riboregulators can be tailor-made to regulate the expression of any target transcript in response to any ligand.

Antisense technologies have been widely utilized to regulate gene expression.<sup>26, 27</sup> We sought to engineer allosteric regulatory functionality by designing a platform on which ligand binding structures were appended to the antisense molecule. In this platform, the antisense domain is sequestered in an “antisense stem” in the absence of ligand. Ligand binding to the aptamer domain mediates a change in the conformational dynamics of the antisense stem that results in the antisense domain being in a more single-stranded form (**Fig. 1a**). Such mechanisms have been described in the construction of signaling aptamers and other allosterically-controlled RNAs.<sup>28</sup>

We constructed an initial antswitch, s1, using a previously selected aptamer that binds the xanthine derivative theophylline with high affinity ( $K_d = 0.29 \mu\text{M}$ ) and specificity.<sup>29</sup> The antisense RNA domain is designed to base pair with a 15 nucleotide region around the start codon of a target mRNA encoding green fluorescent protein (GFP). The stem of the theophylline aptamer is redesigned so that the antisense portion base pairs in a stable stem, the antisense stem, in the absence of ligand, but so that another, overlapping stem forms upon ligand binding, the “aptamer stem”, forcing the antisense portion into a more single-stranded state (**Fig. 1a, b**). The aptamer stem and antisense stem are designed such that the antisense stem is slightly more stable than the aptamer stem. Previous work has demonstrated that the sequence of the lower theophylline aptamer stem is not critical for ligand binding,<sup>30</sup> and this sequence was altered to interact with the antisense stem upon ligand binding. It is anticipated that these molecules will function through alterations in conformational dynamics, such that in the absence of ligand and presence of target transcript, the stem sequestering the antisense is more likely to form; whereas in the presence of both ligand and target transcript, the free energy associated with binding of theophylline (approximately  $8.9 \text{ kcal/mol}^{31}$ ) and RNA stabilization in the aptamer structure enables the aptamer stem to form, freeing the antisense domain to bind its target transcript. RNAstructure<sup>32</sup> was used to predict the stability of the RNA secondary structures formed. Due to the dual-stem design of the antswitch, it is anticipated that the free energies of the aptamer binding to its ligand and the antisense binding to its target mRNA will contribute in a cooperative manner to the structural switching of the antswitch molecule.

The expression of antiswitches in *S. cerevisiae* was accomplished using a novel non-coding RNA (ncRNA) expression construct similar to a previously described system<sup>33</sup> (**Fig. 1c**). Briefly, the RNA to be expressed is cloned between two hammerhead ribozymes known to self-cleave *in vivo*.<sup>34</sup> This dual hammerhead construct can be placed under the control of Pol II promoters, and when transcribed the flanking hammerhead ribozymes cleave out from the desired RNA at an efficiency greater than 99% (**Table 1**). The construct enables creation of ncRNAs with defined 5' and 3' ends that are free of potentially interfering flanking sequences. Antiswitch s1 was expressed in this construct under control of a galactose-inducible (GAL1) promoter in yeast cells. A plasmid containing a yeast enhanced GFP (yEGFP)<sup>35</sup> under the control of a GAL1 promoter was transformed into the same cells (**Fig. 1a**).

Results from protein expression assays demonstrate ligand specific *in vivo* activity of s1 (**Fig. 2a**). Expression of antiswitch s1 in the absence of theophylline decreases GFP expression from control levels by approximately 30%, where addition of greater than 0.8 mM theophylline decreases expression to background levels. The antisense and aptamer domains were expressed separately as controls and had expected effects on GFP expression levels. It is interesting to note the rapid change in expression levels between 0.75 mM and 0.8 mM theophylline. The antiswitch s1 displays binary, on/off behavior rather than linearly modulating expression over a range of theophylline concentrations. This response supports the anticipated cooperative mechanism of structural switching dependent on both ligand and target mRNA. It has been previously demonstrated that the aptamer used in this antiswitch does not bind caffeine,<sup>29</sup> which differs from theophylline by a single methyl group. The addition of caffeine does not change expression levels

from those of an inactive switch, demonstrating that specific ligand-aptamer interactions are necessary to activate the antswitch and free the antisense domain to decrease gene expression of GFP.

Quantitative real-time PCR (qRT-PCR) was performed on antswitch s1 and target mRNA extracted from cells grown under different conditions to determine relative RNA levels (**Table 1**). Relative levels of target transcript did not change significantly between cells harboring s1 grown in the absence and high levels of theophylline, indicating that antswitches function through translational inhibition rather than affecting target RNA levels. In addition, the steady-state relative level of s1 was approximately 1,000-fold that of target levels, although both antswitch and target were expressed from the same promoter. This indicates that antswitch molecules may have higher intracellular stabilities than mRNA potentially due to stabilizing secondary structures or are synthesized more efficiently. The temporal response of antswitch regulation was determined by inducing antswitch activation by the addition of theophylline to cells expressing steady-state levels of GFP and s1 in the “off” state (**Fig. 2b**). GFP levels began decreasing shortly after the addition of theophylline at a rate corresponding to a half-life of approximately .5 to 1 hour, which is consistent with the half-life of the GFP variant used in these experiments.<sup>35</sup> This data supports that antswitch molecules act rapidly to inhibit translation from their target mRNAs in the presence of activating levels of effector and that the time required for target protein levels to decrease is determined by the protein’s half-life.

*In vitro* characterization studies were conducted to examine antiswitch ligand affinity and conformational changes associated with antiswitch response. Gel shift experiments were conducted in the presence of equimolar amounts of a short target transcript (200 nucleotides), containing regions upstream and downstream of the start codon, and labeled s1 and varying concentrations of theophylline to examine antiswitch ligand affinity (**Fig. 2c**). A sharp shift in antiswitch mobility is detected between 2 and 10  $\mu\text{M}$  theophylline, presumably due to binding of both theophylline and target. Nuclease mapping in the presence of ligand alone was also conducted to investigate antiswitch conformational changes (**Fig. 2d**). This data supports that antiswitch molecules exhibit conformational changes at much higher concentrations of ligand than in the presence of ligand and target (between 200  $\mu\text{M}$  and 2 mM versus 2  $\mu\text{M}$  and 10  $\mu\text{M}$ ), supporting the cooperative effects of ligand and target on antiswitch conformational dynamics. The *in vivo* data report the concentration of effector molecule in the media and it is anticipated that the intracellular concentration of these molecules will be much lower due to transport limitations across the membrane. One study reported over a 1,000-fold drop in theophylline concentration across the *E. coli* membrane<sup>36</sup>. The *in vitro* experiments indicate that ligand binding and structural switching occur over narrow concentration ranges, much lower than the extracellular concentrations reported in the *in vivo* studies. This data indicates that in the presence of target *in vitro* antiswitch conformational changes display a sharp binary response to ligand concentrations in the low micromolar range, which is probably indicative of the intracellular concentrations of theophylline in these studies.

The switching behavior of the antiswitch platform is dependent on conformational dynamics of the RNA structures; therefore it is possible to tune switching behavior in a straightforward manner by altering thermodynamic properties of the antiswitch. It is anticipated that the absolute and relative stabilities of the antisense stem and the aptamer stem will be important design parameters in tuning the switch behavior of an antiswitch. To explore the dynamic range of switch behavior, we created several antiswitches (s2–s4) with varying antisense and aptamer stem stabilities (**Fig. 3a**). It was anticipated that these altered antiswitches would expand the concentration range over which the switch in gene expression was observed and increase the dynamic range of GFP expression.

In general, it was observed that increasing antisense stem stability by the addition of base pairs created switches that required higher concentrations of theophylline to affect a switch, whereas decreasing stem stabilities created switches that inhibit GFP expression at lower theophylline concentrations. For example, antiswitch s2 differs from antiswitch s1 by a single nucleotide (A21 to C) (**Fig. 3a**). This mutation introduces a mismatched pair in the antisense stem so that in the absence of ligand, the construct is less thermodynamically stable. As a result, s2 exhibits altered switching dynamics: theophylline concentrations greater than 0.2 mM inhibit gene expression, compared to 0.8 mM for construct s1 (**Fig. 3b**). Alternately, increasing the stability of the antisense stem creates a switch that requires higher concentrations of theophylline to inhibit expression. Antiswitch s3 is designed with an antisense stem five nucleotides longer than s1 and an aptamer stem with 3 bp of the lower stem formed, increasing the absolute stem stabilities. As a result of this increased stability, s3 switches from GFP expression to inhibition of

GFP at approximately 1.25 mM theophylline (**Fig. 3b**), roughly 1.5-fold the concentration required to switch s1 and 6-fold of that required to switch s2. Furthermore, s3 exhibits higher levels of GFP expression in the “off” state, 10% versus 30% inhibition from full expression. Antiswitch s4 was constructed to examine the effects of further destabilizing the antisense stem. This antiswitch includes an altered loop sequence (U18 to C), which further destabilizes the antisense stem from s2. Assays indicate that s4 further expands the dynamic switching behavior of the antiswitch construct, exhibiting switching at 0.1 mM theophylline (**Fig. 3b**).

To demonstrate the modularity of the antiswitch design platform, we constructed and characterized several different antiswitch molecules by swapping in different aptamer domains (**Fig. 4**). These changes in the aptamer domain were designed to keep the antisense stem and the switching aptamer stem identical to previous designs since the target transcript was kept the same, while swapping out the remainder of the aptamer module. To further explore the range of ligand responsiveness in designed antiswitches, we constructed a switch s5 employing a previously characterized aptamer exhibiting lower affinity to theophylline.<sup>29</sup> This aptamer has a  $K_d$  approximately ten-fold higher than the aptamer used in s1–s4. In addition, the response of this antiswitch was tuned by destabilizing the antisense stem in a manner identical to s2, creating s6. To further test the modularity of this platform, an antiswitch was also constructed with a previously characterized aptamer to tetracycline.<sup>37</sup> This aptamer has an affinity to tetracycline similar to that of the theophylline aptamer used in s1–4 ( $K_d = 1 \mu\text{M}$ ).

The data in **Figure 3** support the modularity of the antiswitch platform to different aptamer domains. The modified theophylline aptamers exhibit an altered response to ligand concentrations from s1–4. As expected, the switching for s5 and s6 occurs at higher theophylline concentrations (**Fig. 5a**). Significantly, s5, which contains an aptamer domain with a 10-fold higher  $K_d$  than the aptamer domain in s1, switches at approximately a 10-fold higher theophylline concentration. In addition, the tetracycline antiswitch s7 shows similar switch dynamics as s1–4, suggesting that the response curve observed is a general feature of designed antiswitches (**Fig. 5b**).

To further examine the flexibility of the antiswitch platform, we redesigned the platform in an attempt to construct an “on” antiswitch from the aptamer and antisense domains used in the design of s1. An antiswitch s8 that inhibits expression in the absence of theophylline, but allows expression in the presence of theophylline, was constructed using similar design principles. This switch displays its antisense domain in the absence of ligand, leaving it free to interact with the target mRNA, while sequestering the antisense in the aptamer stem when ligand is present (**Fig. 6a**). s8 displays similar dynamic behavior to s1 (switching around 1 mM theophylline), as is expected due to similar base pairing energetics (**Fig. 6b**). This functional “on” switch demonstrates the flexibility of the antiswitch platform and the generality of the design themes.

The modular nature of the antiswitch platform allows for systems exhibiting combinatorial control over gene expression. To illustrate this, we introduced into cells two switches each responsive to a different effector molecule and each regulating the protein expression of a different mRNA target: s1, a theophylline responsive GFP

regulator, and s9 (see **Fig. 7a** online), a tetracycline responsive yellow fluorescent variant protein (Venus)<sup>38</sup> regulator (**Fig. 7b**). Changes in the targeting capabilities of these molecules were made by swapping out the antisense stem and switching aptamer stem while keeping the remainder of the aptamer module the same. Concurrent expression of these two antiswitches with a plasmid carrying both GFP and Venus allowed for an assay of the simultaneous regulation of gene expression by modular antiswitch design. As shown in **Fig.7c**, addition of theophylline decreased expression of GFP, while Venus expression remained unaffected and addition of tetracycline decreased Venus while not affecting GFP. Furthermore, the addition of both ligands decreased expression of both GFP and Venus. This simple system illustrates the potential of building more complex genetic circuits that are precisely regulated by multiple antiswitch constructs.

This work demonstrates that engineered, ligand controlled antisense RNAs, or antiswitches, are powerful, allosteric regulators of gene expression. The general design of an antiswitch is based on conformational dynamics of RNA folding to create a dual stem molecule comprised of an antisense stem and an aptamer stem. These stems are designed such that in the absence of ligand, the free energy of the antisense stem is lower than that of the aptamer stem. Ligand and target act cooperatively to alter the conformational dynamics of these molecules and stabilize the formation of the aptamer stem and the binding of the antisense domain to its target transcript. The antiswitch platform is flexible, enabling both positive and negative regulation. The “on” switch is designed using the same energetics on an altered platform such that in the absence or low levels of ligand, the antisense domain is free to bind to the target; however, ligand binding changes

the conformational dynamics of these molecules so that the antisense domain is bound in the aptamer stem.

The switching dynamics of antswitch regulators are amenable to tuning by forward engineering design strategies based on thermodynamic properties of RNA. Altering the free energy of the antisense domain alters the conformational dynamics of these molecules in a predictable fashion. Specifically, decreasing the stability of the antisense stem decreases the ligand concentration necessary to switch the antswitch conformation, and increasing the stability of the antisense stem increases the ligand concentration necessary to switch the conformation as well as shifts the dynamics to favor the “off” state at low ligand levels.

In addition, the antswitch platform is fully modular, enabling ligand response and transcript targeting to be engineered by swapping domains within the antswitch molecule. The ligand detection capability of antswitches is designed separately from the targeting capability by swapping only the aptamer domain. Likewise, the targeting capability of these molecules can be designed separately from the ligand detection capability by swapping both the antisense stem and the switching aptamer stem to recognize a different target sequence, while not affecting the aptamer domain.

Antswitch molecules are novel, RNA-based, allosteric regulators of gene expression that can potentially function across a diverse range of organisms, from prokaryotes to humans, making them extremely useful in many different applications. Their design provides a foundation upon which to build other ligand controlled riboregulators for different systems. This type of allosteric riboregulator presents a

powerful tool for gene therapy applications, where one would like to target specific transcripts in response to specific cellular environments that are indicative of a diseased state<sup>39</sup>. One can also anticipate exogenously delivered antiswitches acting as therapeutic molecules, similar to exogenously delivered antisense oligonucleotides, thereby extending the functionality of current antisense therapies by introducing cell-specific action to an already highly targeted therapy. Antiswitch technology can be used to engineer novel regulatory pathways and control loops for applications in metabolic engineering<sup>40</sup> and synthetic circuit design<sup>41</sup> by enabling the cell to sense and respond to intracellular metabolite levels and environmental signals. Finally, antiswitches present new tools for cellular imaging, measuring, and detection strategies, enabling programmable concentration-specific detection of intracellular molecules. Antiswitches offer a unique platform to create tailor-made cellular sensors and “smart” regulators that potentially can target any gene in response to any target ligand, creating new avenues for cellular control and engineering.

## References

1. Banerjee, D. & Slack, F. Control of developmental timing by small temporal RNAs: a paradigm for RNA-mediated regulation of gene expression. *Bioessays*. **24**, 119-129 (2002).
2. Kramer, C., Loros, J.J., Dunlap, J.C. & Crosthwaite, S.K. Role for antisense RNA in regulating circadian clock function in *Neurospora crassa*. *Nature*. **421**, 948-952 (2003).
3. Ellington, A.D. & Szostak, J.W. In vitro selection of RNA molecules that bind specific ligands. *Nature*. **346**, 818-822 (1990).
4. Tuerk, C. & Gold, L. Systematic evolution of ligands by exponential enrichment: RNA ligands to bacteriophage T4 DNA polymerase. *Science*. **249**, 505-510 (1990).
5. Good, L. Diverse antisense mechanisms and applications. *Cell. Mol. Life Sci.* **60**, 823-824 (2003).
6. Good, L. Translation repression by antisense sequences. *Cell. Mol. Life Sci.* **60**, 854-861 (2003).

7. Vacek, M., Sazani, P. & Kole, R. Antisense-mediated redirection of mRNA splicing. *Cell. Mol. Life Sci.* **60**, 825-833 (2003).
8. Bartel, D.P. MicroRNAs: genomics, biogenesis, mechanism, and function. *Cell.* **116**, 281-297 (2004).
9. Scherer, L. & Rossi, J.J. Recent applications of RNAi in mammalian systems. *Curr. Pharm. Biotechnol.* **5**, 355-360 (2004).
10. Lilley, D.M. The origins of RNA catalysis in ribozymes. *Trends Biochem. Sci.* **28**, 495-501 (2003).
11. Mandal, M. & Breaker, R.R. Adenine riboswitches and gene activation by disruption of a transcription terminator. *Nat. Struct. Mol. Biol.* **11**, 29-35 (2004).
12. Winkler, W., Nahvi, A. & Breaker, R.R. Thiamine derivatives bind messenger RNAs directly to regulate bacterial gene expression. *Nature.* **419**, 952-956 (2002).
13. Winkler, W.C., Nahvi, A., Roth, A., Collins, J.A. & Breaker, R.R. Control of gene expression by a natural metabolite-responsive ribozyme. *Nature.* **428**, 281-286 (2004).
14. Barrick, J.E. et al. New RNA motifs suggest an expanded scope for riboswitches in bacterial genetic control. *Proc. Natl. Acad. Sci. USA.* **101**, 6421-6426 (2004).
15. Yelin, R. et al. Widespread occurrence of antisense transcription in the human genome. *Nat. Biotechnol.* **21**, 379-386 (2003).
16. Lavorgna, G. et al. In search of antisense. *Trends Biochem. Sci.* **29**, 88-94 (2004).
17. Hermann, T. & Patel, D.J. Adaptive recognition by nucleic acid aptamers. *Science.* **287**, 820-825 (2000).
18. Cox, J.C. et al. Automated selection of aptamers against protein targets translated in vitro: from gene to aptamer. *Nuc. Acids Res.* **30**, e108 (2002).
19. Jhaveri, S., Rajendran, M. & Ellington, A.D. In vitro selection of signaling aptamers. *Nat. Biotechnol.* **18**, 1293-1297 (2000).
20. Roth, A. & Breaker, R.R. Selection in vitro of allosteric ribozymes. *Methods Mol. Biol.* **252**, 145-164 (2004).
21. Stojanovic, M.N. & Kolpashchikov, D.M. Modular aptameric sensors. *J. Am. Chem. Soc.* **126**, 9266-9270 (2004).
22. Smolke, C.D., Carrier, T.A. & Keasling, J.D. Coordinated, differential expression of two genes through directed mRNA cleavage and stabilization by secondary structures. *Appl Environ Microbiol.* **66**, 5399-5405 (2000).
23. Isaacs, F.J. et al. Engineered riboregulators enable post-transcriptional control of gene expression. *Nat. Biotechnol.* **22**, 841-847 (2004).
24. Yen, L. et al. Exogenous control of mammalian gene expression through modulation of RNA self-cleavage. *Nature.* **431**, 471-476 (2004).
25. Buskirk, A.R., Landrigan, A. & Liu, D.R. Engineering a ligand-dependent RNA transcriptional activator. *Chem. Biol.* **11**, 1157-1163 (2004).
26. Weiss, B., Davidkova, G. & Zhou, L.W. Antisense RNA gene therapy for studying and modulating biological processes. *Cell. Mol. Life Sci.* **55**, 334-358 (1999).
27. Scherer, L.J. & Rossi, J.J. Approaches for the sequence-specific knockdown of mRNA. *Nat. Biotechnol.* **21**, 1457-1465 (2003).
28. Nutiu, R. & Li, Y. Structure-switching signaling aptamers. *J. Am. Chem. Soc.* **125**, 4771-4778 (2003).

29. Zimmermann, G.R., Wick, C.L., Shields, T.P., Jenison, R.D. & Pardi, A. Molecular interactions and metal binding in the theophylline-binding core of an RNA aptamer. *RNA*. **6**, 659-667 (2000).
30. Zimmermann, G.R., Jenison, R.D., Wick, C.L., Simorre, J.P. & Pardi, A. Interlocking structural motifs mediate molecular discrimination by a theophylline-binding RNA. *Nat. Struct. Biol.* **4**, 644-649 (1997).
31. Gouda, H., Kuntz, I.D., Case, D.A. & Kollman, P.A. Free energy calculations for theophylline binding to an RNA aptamer: Comparison of MM-PBSA and thermodynamic integration methods. *Biopolymers*. **68**, 16-34 (2003).
32. Mathews, D.H. et al. Incorporating chemical modification constraints into a dynamic programming algorithm for prediction of RNA secondary structure. *Proc. Natl. Acad. Sci. USA*. **101**, 7287-7292 (2004).
33. Taira, K., Nakagawa, K., Nishikawa, S. & Furukawa, K. Construction of a novel RNA-transcript-trimming plasmid which can be used both in vitro in place of run-off and (G)-free transcriptions and in vivo as multi-sequences transcription vectors. *Nuc. Acids Res.* **19**, 5125-5130 (1991).
34. Samarsky, D.A. et al. A small nucleolar RNA:ribozyme hybrid cleaves a nucleolar RNA target in vivo with near-perfect efficiency. *Proc. Natl. Acad. Sci. USA*. **96**, 6609-6614 (1999).
35. Mateus, C. & Avery, S.V. Destabilized green fluorescent protein for monitoring dynamic changes in yeast gene expression with flow cytometry. *Yeast*. **16**, 1313-1323 (2000).
36. Koch, A.L. The metabolism of methylpurines by *Escherichia coli*. I. Tracer studies. *J. Biol. Chem.* **219**, 181-188 (1956).
37. Berens, C., Thain, A. & Schroeder, R. A tetracycline-binding RNA aptamer. *Bioorg. Med. Chem.* **9**, 2549-2556 (2001).
38. Nagai, T. et al. A variant of yellow fluorescent protein with fast and efficient maturation for cell-biological applications. *Nat. Biotechnol.* **20**, 87-90 (2002).
39. Watkins, S.M. & German, J.B. Metabolomics and biochemical profiling in drug discovery and development. *Curr. Opin. Mol. Ther.* **4**, 224-228 (2002).
40. Khosla, C. & Keasling, J.D. Metabolic engineering for drug discovery and development. *Nat. Rev. Drug Discov.* **2**, 1019-1025 (2003).
41. Kobayashi, H. et al. Programmable cells: interfacing natural and engineered gene networks. *Proc. Natl. Acad. Sci. USA*. **101**, 8414-8419 (2004).
42. Sambrook, J. & Russell, D.W. *Molecular cloning: A laboratory manual*, Edn. 3rd. (Cold Spring Harbor Laboratory Press, Cold Spring Harbor, NY; 2001).
43. Sikorski, R.S. & Hieter, P. A system of shuttle vectors and yeast host strains designed for efficient manipulation of DNA in *Saccharomyces cerevisiae*. *Genetics*. **122**, 19-27 (1989).
44. Gietz, R. & Woods, R. in *Guide to Yeast Genetics and Molecular and Cell Biology*, Part B, Vol. 350. (eds. C. Guthrie & G. Fink) 87-96 (Academic Press, San Diego; 2002).
45. Caponigro, G., Muhlrad, D. & Parker, R. A small segment of the MAT alpha 1 transcript promotes mRNA decay in *Saccharomyces cerevisiae*: a stimulatory role for rare codons. *Mol. Cell. Biol.* **13**, 5141-5148 (1993).





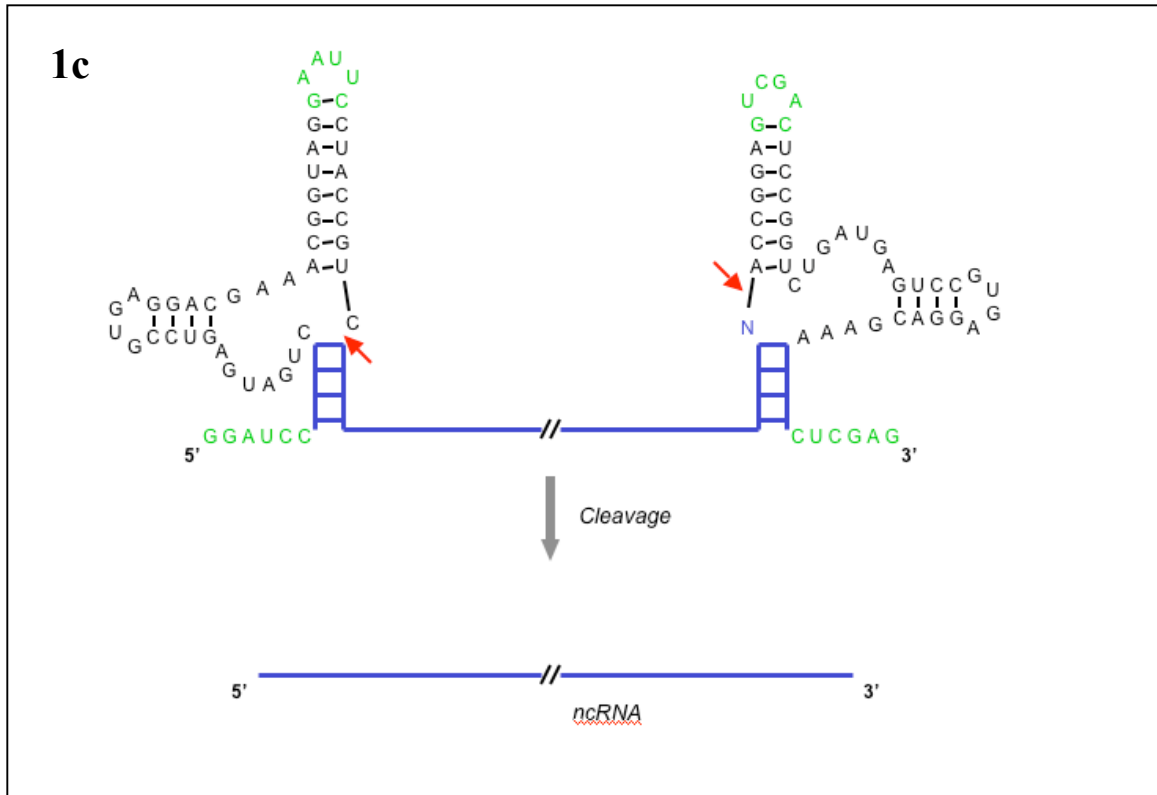


**Figure 1 Design and function of a novel antiswitch regulator. (a)** General illustration of the mechanism by which an antiswitch molecule acts to regulate gene expression *in vivo*. The antisense sequence is indicated in red; switching “aptamer stem” is shown in blue. In the absence of effector, the antisense domain is bound in a double-stranded region of the RNA referred to as the “antisense stem” and the antiswitch is in the “off” state. In this state the antiswitch is unable to bind to its target transcript, which encodes a *gfp* coding region, and as a result, GFP production is on. In the presence of effector, the antiswitch binds the molecule, forcing the aptamer stem to form, switching its confirmation to the “on” state. In this state the antisense domain of the antiswitch will bind to its target transcript and through an antisense mechanism turn the production of GFP off. **(b)** Sequence and predicted structural switching of a theophylline-responsive

antiswitch, s1, and its target mRNA. On s1, the antisense sequence is indicated in red; switching aptamer stem sequence is indicated in blue, the stability of each switching stem is indicated. On the target mRNA, the start codon is indicated in green. (c) Sequence and cleavage mechanism of ncRNA expression construct. The expression construct enables cloning of general sequences between two hammerhead ribozyme sequences through unique restriction sites *Bam*HI, *Eco*RI, *Sal*I, and *Xho*I (indicated in green). Predicted cleavage sites are indicated by red arrows. General ncRNA insert is indicated by a blue line or lettering. Following cleavage, the resulting ncRNA has defined 3' and 5' ends.

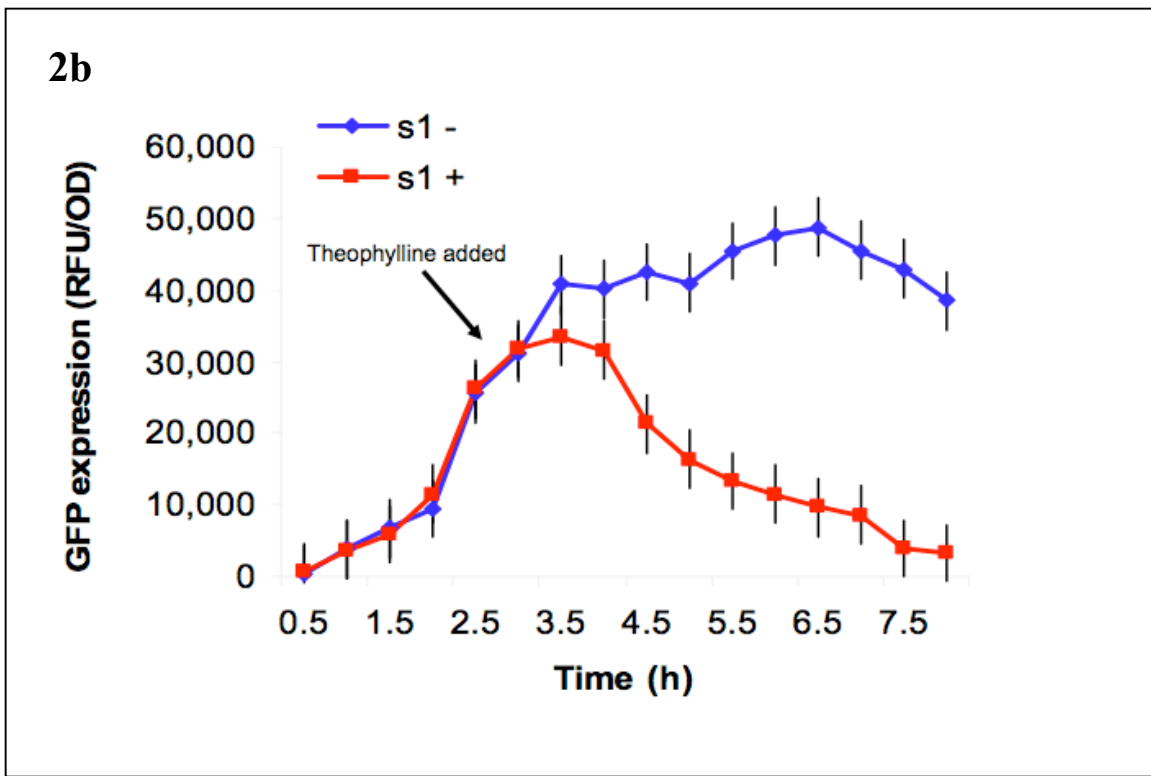
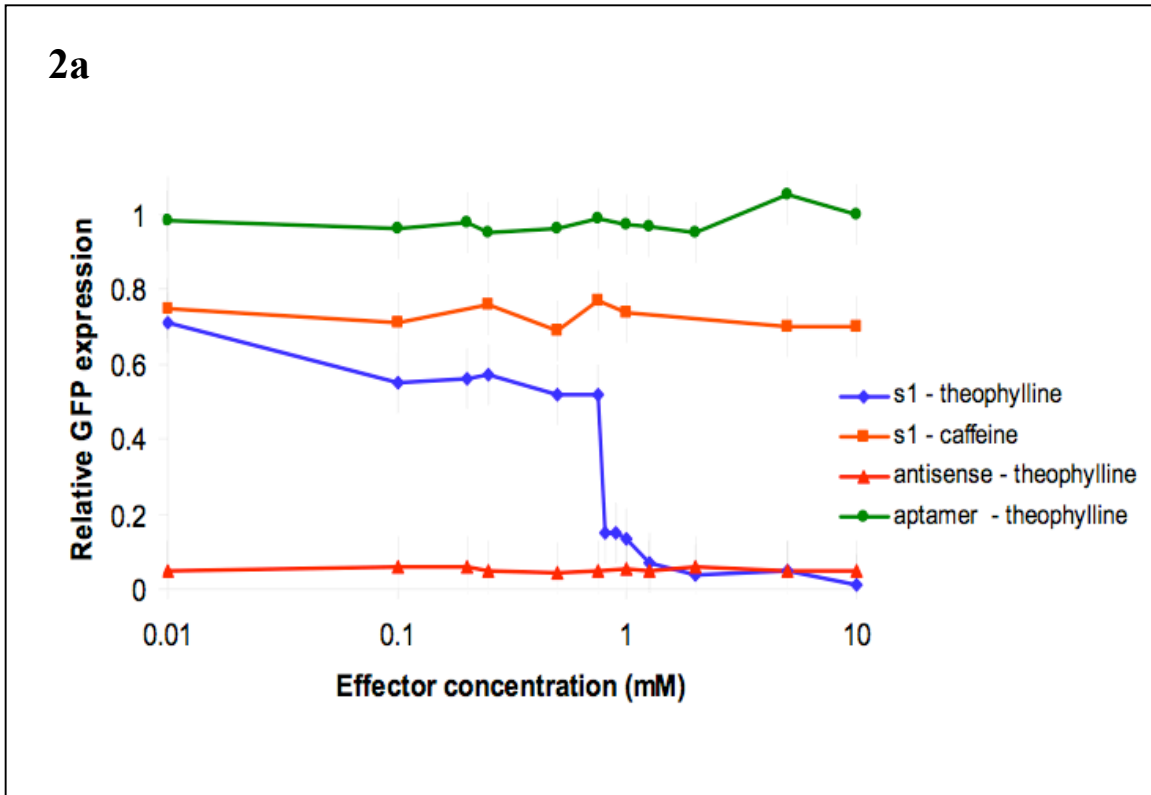


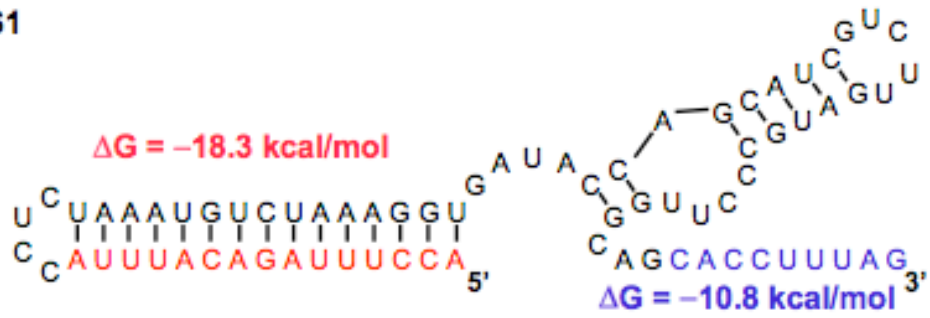


**Figure 2 (a)** *In vivo* GFP regulation activity of s1 and controls across different effector concentrations: aptamer construct (negative control) in the presence of theophylline (green); antisense construct (positive control) in the presence of theophylline (red); s1 in the presence of caffeine (negative control, orange); s1 in the presence of theophylline (blue). Data is presented as relative, normalized GFP expression in cells harboring these constructs against expression levels from induced and uninduced cells harboring only the GFP expression construct. **(b)** *In vivo* temporal response of s1 inhibiting GFP expression upon addition of effector to cells that have accumulated steady-state levels of GFP and antiswitch s1: no theophylline (blue); 2 mM theophylline (red). **(c)** *In vitro* affinity assays of s1 to target and effector molecules. The mobility of radiolabeled s1 was monitored in the presence of equimolar concentrations of target transcript and varying concentrations of theophylline as indicated. **(d)** Structural probing of antiswitch s1 through nuclease mapping. Samples correspond to fluorescently labeled s1 incubated in the presence of RNase T1 and varying concentrations of theophylline. Fragments generated by RNase T1 cleavage 3' of single-stranded G's were separated by capillary electrophoresis. Peak 1 corresponds to the antisense domain, and peak 2 corresponds to the switching aptamer stem. In both the absence of theophylline and 200  $\mu$ M theophylline, the switching aptamer stem is cleaved (peak 2), indicating that this domain is in a single-stranded form, accessible to the nuclease. In 2 mM theophylline this peak is absent, indicating that the aptamer stem is protected in a double-stranded stem. Furthermore, in 2 mM theophylline the disappearance of peak 2 occurs simultaneously with the appearance of peak 1, indicating that the antisense domain is in a single-stranded form accessible to the

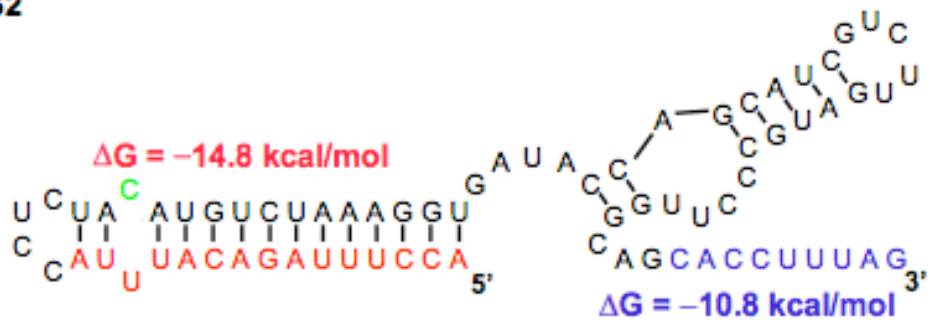
nuclease. This peak is not present in lower levels of theophylline, supporting a change in accessibility of this region of the antiswitch under these concentrations. Unlabeled peaks between 1 and 2 correspond to cleavage within the region connecting the antisense and aptamer stems. Peaks after 2 correspond to full-length constructs.

3a

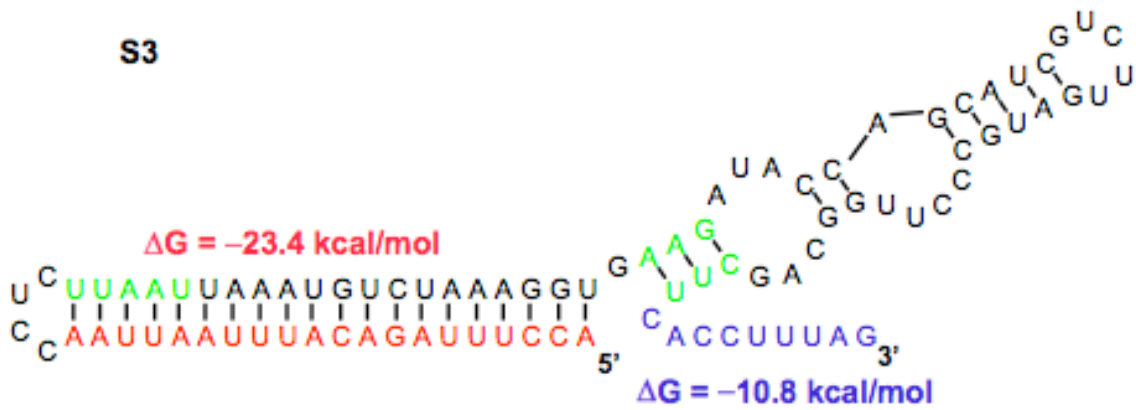
S1



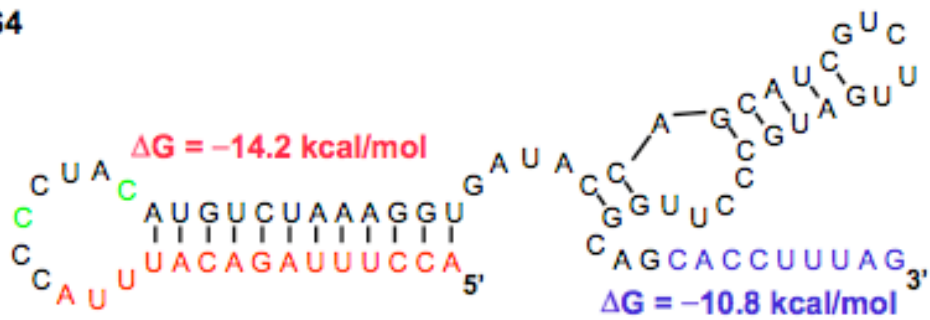
S2



S3



S4



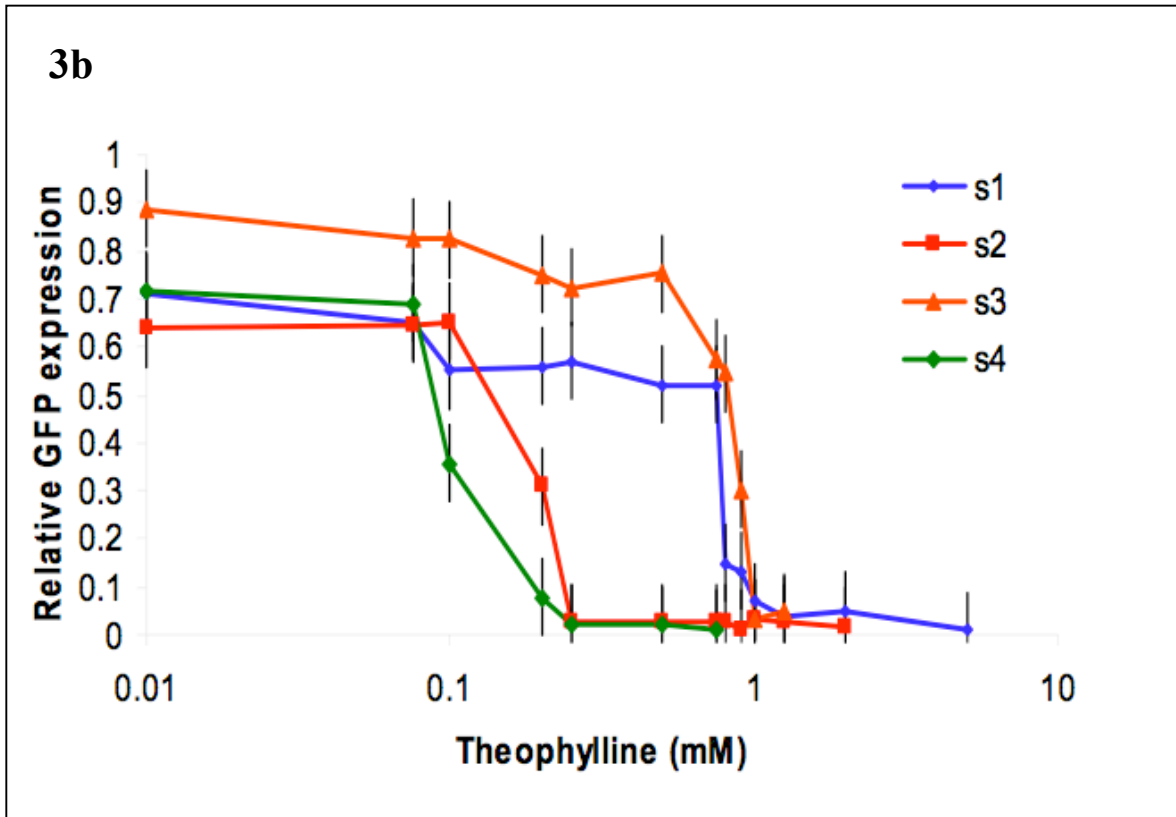


**Figure 3** Tuning and expanding the switch response of an antiswitch regulator. **(a)** Predicted structures of tuned antiswitches (s2–s4), based on s1, in the absence of theophylline binding. The antisense sequences are indicated in red; switching aptamer stem sequences are indicated in blue; modified sequences are indicated in green, the stability of each switching stem is indicated. **(b)** *In vivo* GFP regulation activity of s1s4 across different theophylline concentrations: s1- initial antiswitch construct (blue); s2- destabilized antiswitch construct (red); s3- stabilized antiswitch construct (orange); s4- destabilized antiswitch construct (green).

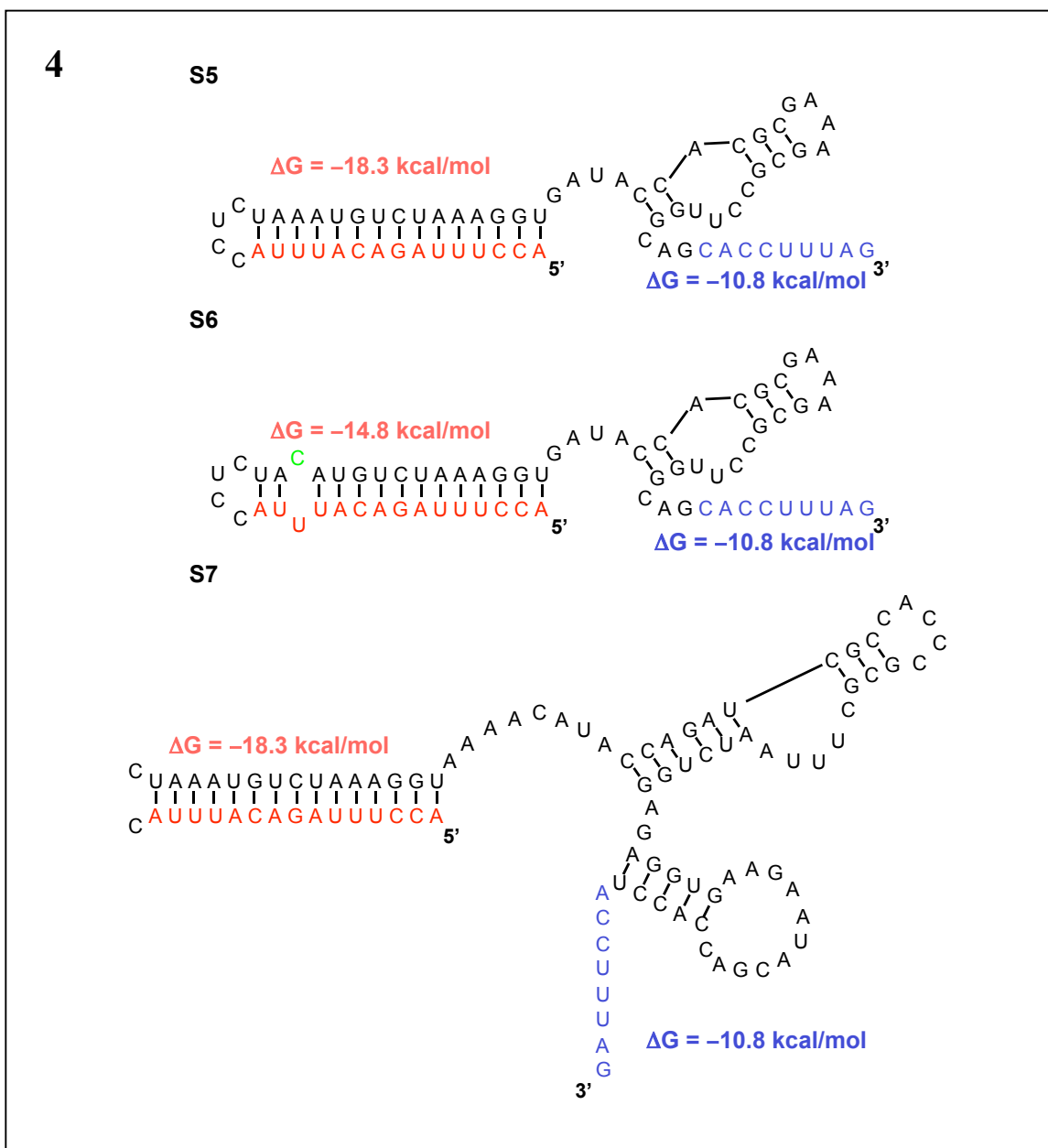


**Figure 4.** Sequences and predicted structures of antiswitches s5, s6, and s7 in the absence of ligand binding. The antisense sequences are indicated in red; switching aptamer stem sequences are indicated in blue; modified sequences are indicated in green; the stability of each switching stem is indicated: s5- modified theophylline aptamer antiswitch based on s1; s6- destabilized modified theophylline aptamer antiswitch; s7- tetracycline aptamer antiswitch based on s1.

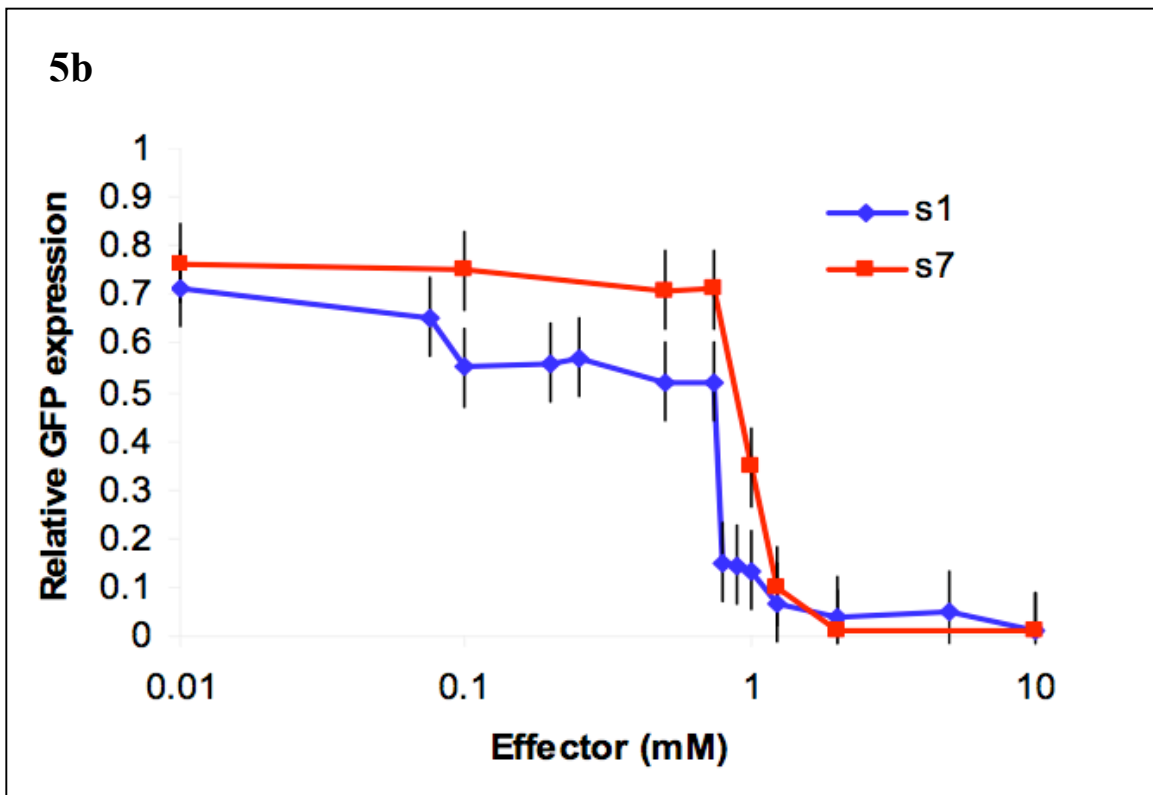
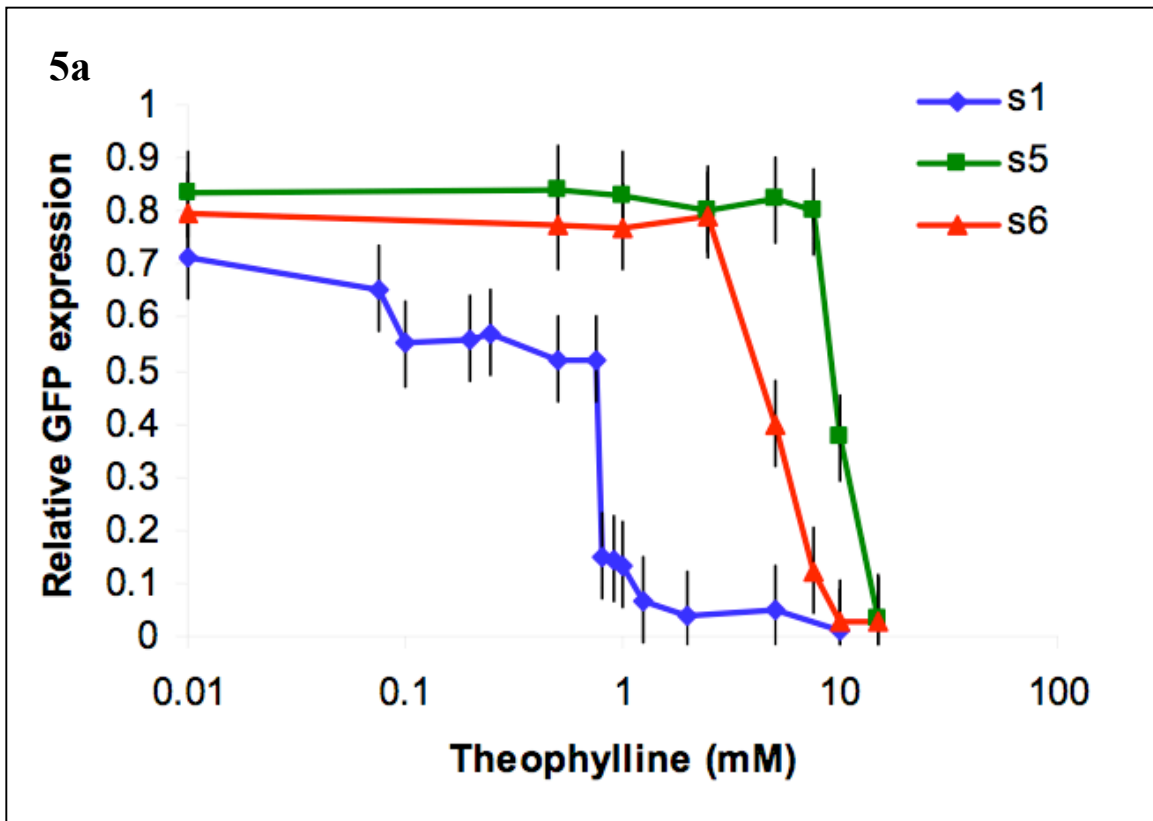


**Figure 5. (a)** *In vivo* GFP regulation activity of modified aptamer-antiswitch constructs (s5–s6) across different theophylline concentrations: s1- initial antiswitch construct (blue); s5- antiswitch construct with an aptamer domain having 10-fold lower affinity to theophylline than that used in s1 (green); s6- destabilized modified aptamer-antiswitch construct, based on s5 (red). **(b)** *In vivo* GFP regulation activity of antiswitch constructs responsive to different small molecule effectors (s1, s7) across different effector concentrations: s1- initial antiswitch construct responsive to theophylline (blue); s7- antiswitch construct modified with a tetracycline aptamer domain, based on s1, responsive to tetracycline (red).

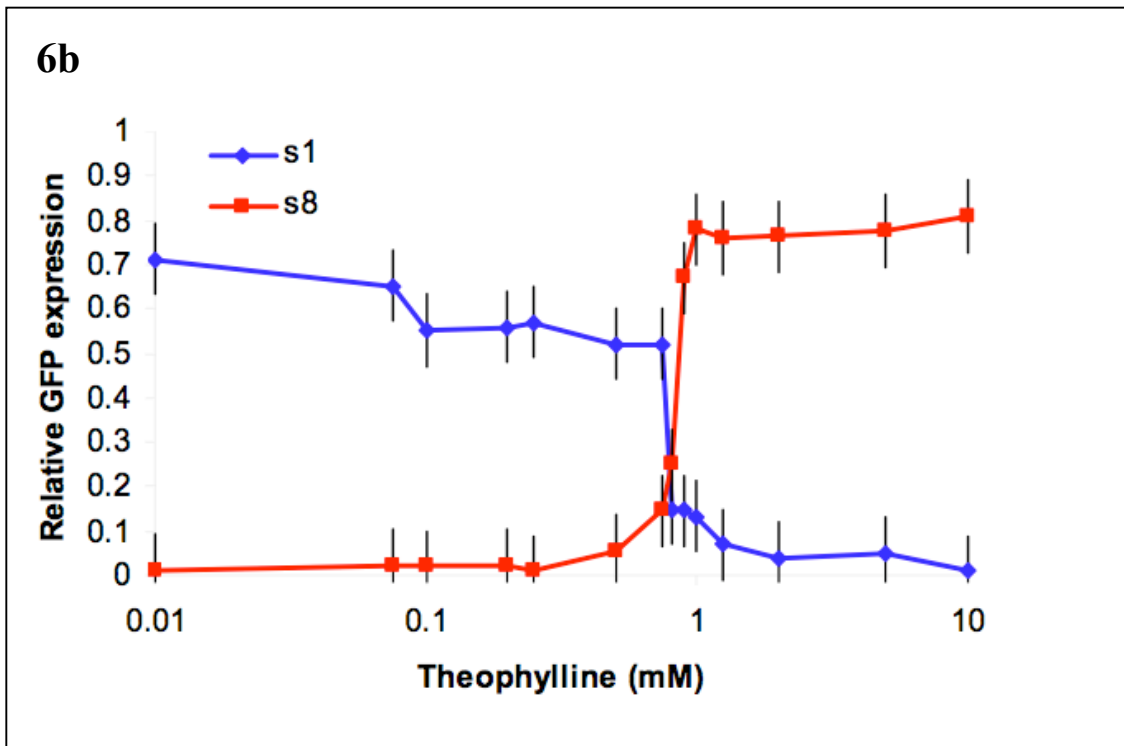
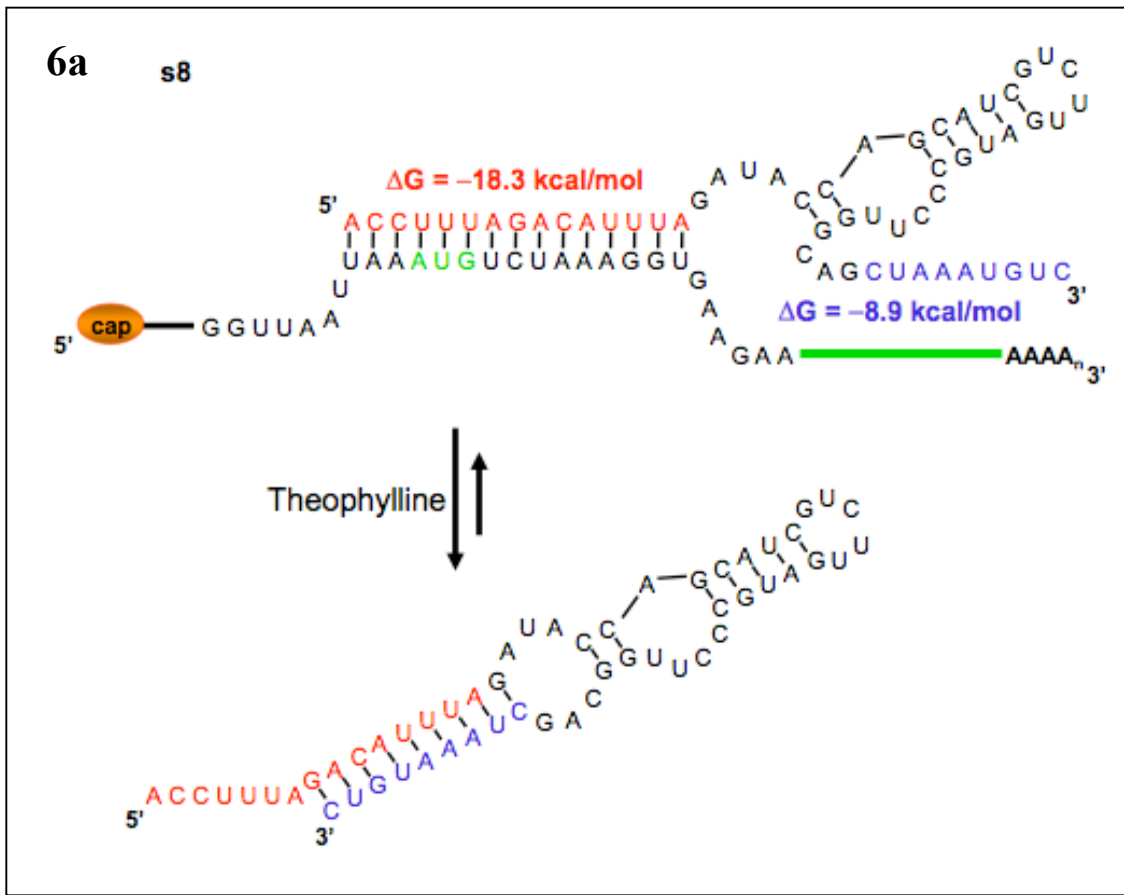


**Figure 6** Redesign and characterization of a novel “on” antswitch regulator. **(a)** Sequence and structural switching of an “on” antswitch regulator (s8) responsive to theophylline. The antisense sequence is indicated in red; switching aptamer stem sequence is indicated in blue; the stability of each switching stem is indicated. On the target mRNA, the start codon is indicated in green. s8 is designed such that in the absence of theophylline, the antswitch is “on” or the antisense domain is free to bind to its target. In the presence of theophylline, the antswitch undergoes a conformational change to the “off” state such that the antisense domain is bound in a double-stranded RNA stem that is part of the aptamer stem. **(b)** *In vivo* GFP regulation activity of “on” and “off” antswitch constructs across different theophylline concentrations: s1- initial ‘off’ antswitch construct (blue); s8- redesigned “on” antswitch construct, based on s1 (red).



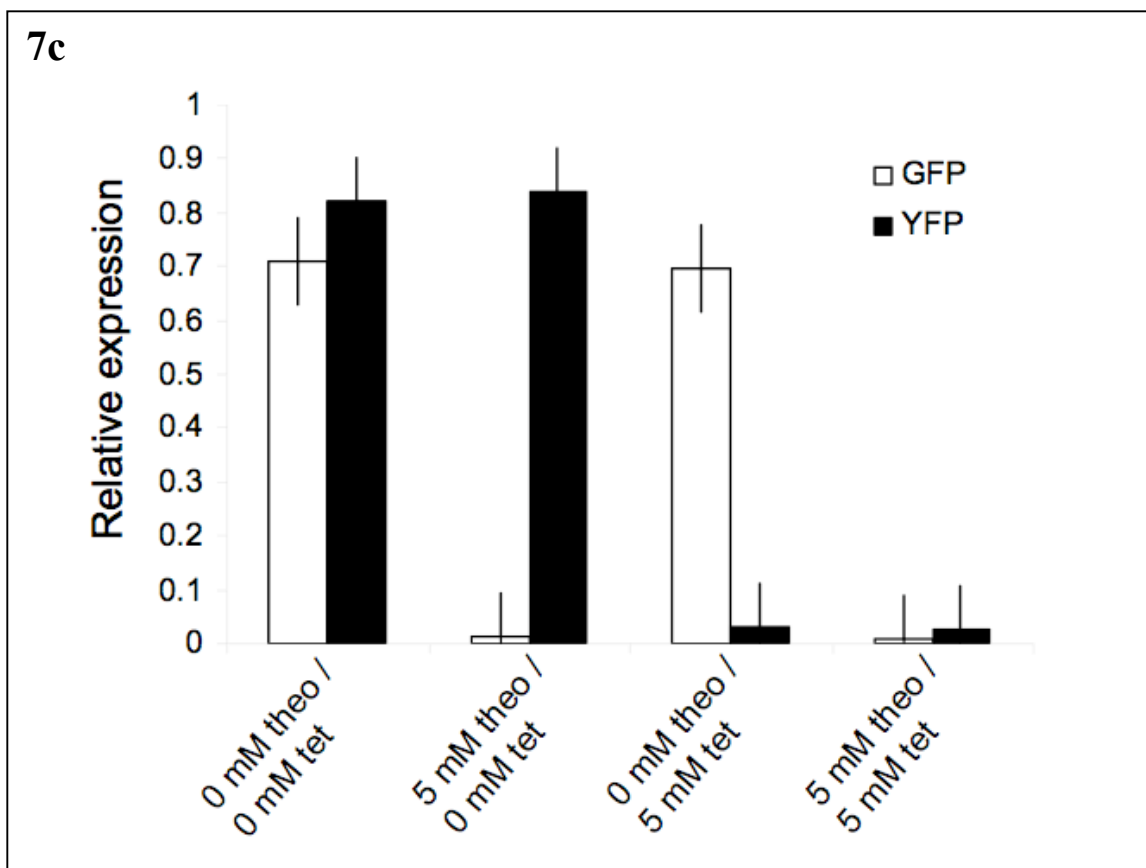


**Figure 7.** (a) Sequence and structural switching of a tetracycline-responsive Venus (YFP) regulator, s9, and its target mRNA. On s9, the antisense sequence is indicated in red; switching aptamer stem sequence is indicated in blue, the stability of switching stem is indicated. On the target mRNA, the start codon is indicated in green. (b) Illustration of the mechanism by which two independent antswitch molecules act to regulate the expression of multiple target genes *in vivo*. In the absence of their respective effectors, the antswitches are in the “off” state and are unable to bind to their target transcripts. In this state, both GFP and YFP production is on. In the presence of theophylline, one antswitch switches its conformation to the “on” state and turns off GFP production. In the presence of tetracycline, the second antswitch switches its conformation to the “on”

state and turns off YFP production. These antiswitches act independently of each other to provide combinatorial control over genetic circuits. **(c)** *In vivo* regulation activity of two antiswitch constructs (s1, s9) against their respective targets (GFP, YFP) in the presence or absence of their respective effector molecules (theophylline, tetracycline). Relative YFP expression (black); relative GFP expression (white).

**Table 1** Relative RNA levels of target mRNA and antiswitch s1. Relative levels are normalized to GFP mRNA levels in the absence of theophylline.

RNA	0 mM theophylline	2 mM theophylline
GFP mRNA	1±0.048	1.1±0.052
Antiswitch s1	990±46.2	971±47.1
Uncleaved hammerhead	0.158±0.009	0.149±0.008

Antiswitch construct	RNA sequence
s1	ACCUUUAGACAUUUACCUCUAAAUGUCUAAAGGUGAUACCAGCAUCGUCUUGAUGCCCUUGGCAGCACCUUUAG
s2	ACCUUUAGACAUUUACCUCUACAUGUCUAAAGGUGAUACCAGCAUCGUCUUGAUGCCCUUGGCAGCACCUUUAG
s3	ACCUUUAGACAUUUAAUUAACCUCUAAAUAAAUGUCUAAAGGUGAAGAUACCAGCAUCGUCUUGAUGCCCUUGGCAGCUUACCUUUAG
s4	ACCUUUAGACAUUUACCCUACAUGUCUAAAGGUGAUACCAGCAUCGUCUUGAUGCCCUUGGCAGCACCUUUAG
s5	ACCUUUAGACAUUUACCUCUAAAUGUCUAAAGGUGAUACCACGCGAAAGCGCCUUGGCAGCACCUUUAG
s6	ACCUUUAGACAUUUACCUCUACAUGUCUAAAGGUGAUACCACGCGAAAGCGCCUUGGCAGCACCUUUAG
s7	ACCUUUAGACAUUUACCUCUAAAUGUCUAAAGGUAACAACCAUACCAGCAUCGCCACCCGCGUUAAUCUGGAGAGGUGAAGAAUACGACCACCUACCUUUAG
s8	ACCUUUAGACAUUUAGAUACCAGCAUCGUCUUGAUGCCCUUGGCAGCUAAAUGUC
s9	UUGCUCACCAUGGUCCACCAUGGUGAGCAAAAAACAUACCAGAUCCGCCACCCGCGUUAAUCUGGAGAGGUGAAGAAUACGACCACCUUUGCUCAC
GFP antisense	ACCUUUAGACAUUU
Theophylline aptamer	AGGUGAUACCAGCAUCGUCUUGAUGCCCUUGGCAGCACCU
s1.qpcr.fwd	ACCAGACAACCCAAAGCAA
s1.qpcr.rev	CTAAAGGTGCTGCCAAGGG
s1/2ham.qpcr.fwd	TAGCGGATCCAGGTCTGATGAGTCCGTGAGGACG
gfp.qpcr.fwd	ATTTTGGTTGAATTAGATGGTGA
gfp.qpcr.rev	CTGGCAATTTACCAGTAGTACAAA

<b>Plasmid</b>	<b>Description</b>	<b>Parent plasmid</b>
pTARGET1.gfp	pRS314-Gal expressing yEGFP	pRS314-Gal
pTARGET2.gfp/V	pRS314-Gal expressing yEGFP and Venus	pRS314-Gal
pSWITCH1.s1	GAL1 / ribozyme construct expressing s1	pRS316-Gal
pSWITCH1.s2	GAL1 / ribozyme construct expressing s2	pRS316-Gal
pSWITCH1.s3	GAL1 / ribozyme construct expressing s3	pRS316-Gal
pSWITCH1.s4	GAL1 / ribozyme construct expressing s4	pRS316-Gal
pSWITCH1.s5	GAL1 / ribozyme construct expressing s5	pRS316-Gal
pSWITCH1.s6	GAL1 / ribozyme construct expressing s6	pRS316-Gal
pSWITCH1.s7	GAL1 / ribozyme construct expressing s7	pRS316-Gal
pSWITCH1.s8	GAL1 / ribozyme construct expressing s8	pRS316-Gal
pSWITCH2.s1/9	GAL1 / ribozyme construct expressing s1 and s9	pRS316-Gal
pSWITCH1.anti	GAL1 / ribozyme construct expressing GFP antisense	pRS316-Gal
pSWITCH1.apramer	GAL1 / ribozyme construct expressing theophylline aptamer	pRS316-Gal